Appl Biochem Biotechnol (2011) 163:882–894
DOI 10.1007/s12010-010-9092-z

Characterization of Biosorption Process of Acid Orange 7 on Waste Brewery's Yeast

YunHai Wu · Yue Hu · ZhengWei Xie · ShiXun Feng · Bin Li · XianMiao Mi

Received: 30 November 2009 / Accepted: 9 September 2010 /
Published online: 19 September 2010

Abstract The use of cheap, high-efficiency, and ecofriendly adsorbent has been studied as an alternative way for the removal of dyes from wastewater. This paper investigated the use of waste brewery's yeast for the removal of acid orange 7 from aqueous solution. The optimum removal of acid orange 7 was found to be 3.561 mg/g at pH 2.0, 10 mg/L initial concentration and 303 K. The kinetic studies indicated that the biosorption process of acid orange 7 agreed well with the pseudo-second-order model. The external diffusion is the rate-controlling step of the initial fast adsorption (<20 min) and then the intraparticle diffusion dominated the mass transfer process. Langmuir, Freundlich, and Dubinin–Radushkevich models were applied to describe the biosorption isotherm of acid orange 7 by waste brewery's yeast. Langmuir isotherm model fits the equilibrium data, at all the studied temperatures, better than the other isotherm models which indicates monolayer dye biosorption process. The highest monolayer biosorption capacity was found to be 2.27×10^{-3} mol/g at 303 K. The calculated thermodynamic parameters (ΔG, ΔS, ΔH) showed the biosorption process to be spontaneous and exothermic in nature. Amine or amino, amide, carboxyl, phosphate groups are responsible for the dyes biosorption based on the result of Fourier transform infrared analysis.

Keywords Biosorption · Waste brewer's yeast · Acid orange 7 · Thermodynamic

Introduction

Nowadays, environment pollution has become a matter of great concern in our society. Most of the environmental pollutions are related to the industrial pollutions. Dyes as an important industrial product, have been widely used in textile, leather, paper, food, and other industries. According to statistics, the world's annual production of dyes is 8×10^6 t, and at least 10% of which enter into the natural water bodies [1]. The discharge of these dyes may significantly affect photosynthetic activity in aquatic life by reducing light

Y. Wu · Y. Hu (✉) · Z. Xie · S. Feng · B. Li · X. Mi
College of Environmental Science and Engineering, Hohai University, Nanjing 210098, China
e-mail: huyue002@yahoo.cn

penetration [2, 3]. Furthermore, the dye bearing effluents are considered to be a very complex and inconsistent mixture of many pollution substances ranging from organic-chlorine-based pesticides to heavy metals and is considered to be recalcitrant and non-biodegradable [4]. So the removal of dyes from water body has draw great attention within environmental research [5]. Dye wastewater is usually treated by physical or chemical treatment processes. These include chemical coagulation/flocculation, ozonation, photooxidation, ion exchange, irradiation, precipitation, and adsorption. Although they can remove dyes partially, various limitations prevent them to be economical and thus cannot be used widely and economically [6–8]. Currently, activated carbon is often as a sorbent to remove dyes in wastewater because of its excellent adsorption ability. However, the technology for manufacturing good quality activated carbon is still very cost-prohibitive and the regeneration or disposal of the spent carbon is often problematic. This has prompted the use of cheap and efficient alternative substitutes to remove dyes from wastewater. Some of these alternative adsorbents are palm ash and chitosan/oil palm ash [9, 10], shale oil ash [11], pomelo (*Citrus grandis*) peel [12], de-oiled soya and bottom ash [13], sunflower seed shells and mandarin peelings [14], wheat husk [15, 16], guava leaf powder [17], and steel and fertilizer industries wastes [18].

Waste brewery's yeast (WBY), a by-product from brewing industry, could be a new alternative for wastewater processes. Because of the prosperous market of the brewing industry, the production of this material has steadily increased during the past years. The ability of the waste yeast as biosorbent for heavy metals has been recognized [19–21]. However, there have been few researches on biosorption of dyes on waste brewery's yeast. The aim of this study is to investigate the potentiality of WBY for removing of acid orange 7 (AO7) from aqueous solution. The effects of solution pH, contact time, initial dye concentration, and temperature on AO7 adsorption were investigated. Moreover, the biosorption kinetics, isotherms, thermodynamic, and the mechanisms of dyes biosorption on WBY were discussed.

Materials and Methods

Materials

Waste brewery's yeast employed in this study is taken from Jinling Beer Company in Nanjing, Jiangsu province, China. It was washed with large amount of deionized water. Then it was centrifuged and the supernatant was discarded. This process was repeated three times to remove the adsorbed nutrient ions. The biomass was dried in an oven (333 K for 12 h) and then powdered to particles using a mortar and pestle. The powdered biomass was then screened through a sieve (120 meshes) to select particles of less than 0.125 mm which was stocked in the desiccators.

Acid orange 7(C.I. 15510) was obtained from Nanjing RuiTai chemical reagents Ltd. The chemical structure of AO7 was shown in Fig. 1.

The dye concentrations were determined by measuring the absorbency at the maximum wavelength 486 nm and then calculated according to the calibration curve.

Batch Studies

Adsorption experiments were carried out by adding a fixed amount of WBY(0.1 g) to 50 mL dye solution at concentrations ranging from 10 to 500 mg/L, pH ranging from 1.0 to

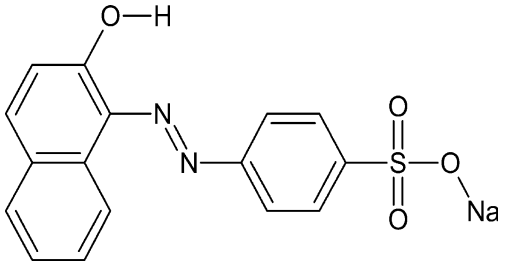

Fig. 1 Chemical structure of AO7

10.0 and the temperature ranging from 293 to 313 K in a series of 250 mL conical flasks in a temperature controlled shaker. The agitation speed of the shaker was fixed at 120 rpm for all batch experiments. The samples were taken at intervals (5, 10, 20, 40, 60, 100, 240, 360 min) for kinetics study. Then the samples were centrifuged immediately at the speed of 8,000 rpm and the dye in the supernatant was analyzed. The amount of the dye adsorbed (mg) per unit mass of biomass (g), q_e was obtained by mass balance using the equation:

$$q_e = \frac{(C_0 - C_e)V}{M} \tag{1}$$

Where C_0 and C_e are initial and equilibrium concentrations of the dye (mg/L), respectively, M is the weight of dry biomass (g), and V is the volume of the solution (L).

Infrared Spectra Analysis

To investigate the main functional groups responsible for dye adsorption and the chemical nature of the binding process. The dried biomass and dye bound biomass were analyzed by Fourier transform infrared (FT-IR) spectroscopy by preparing the biomass pellets in KBr.

Results and Discussion

Effect of pH

The pH value of the solution is an important controlling parameter in the adsorption process, and the initial pH value of the solution has more influence than the final pH, which influences both the cell surface dye binding sites and the dye chemistry in water [22]. As shown in the Fig. 2, with the increase of pH, adsorption was found to decrease till pH 5.0 and beyond pH 5.0, no significant difference in the amount of dye adsorbed was observed on proceeding further till pH 10.0.

The decrease in adsorption by increasing pH can be explained by protonation and deprotonation [23], and AO7 is an anionic dye, on addition of acid, some groups on the surface of WBY such as amine, amino, etc. have been protonated because of the abundance of H^+, making the surface of WBY with positive charge, which can adsorb the anionic dye AO7. With increase of pH, deprotonation of the dye takes place, and when the pH value continues to rise, the carboxyl, phosphate, etc. on the surface of WBY will be in anionic form, thus making the surface of WBY with negative charge. Due to the electrostatic repulsion, the anionic dye combined to the groups on WBY difficultly, which thereby

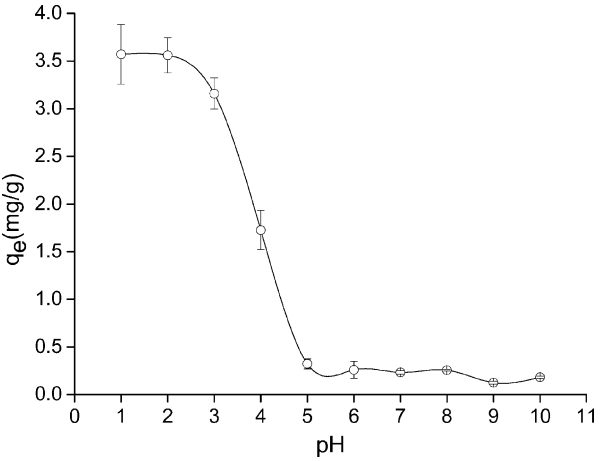

Fig. 2 Effect of pH on the adsorption of AO7on WBY at T=303 K, initial concentration: 10 mg/L

decreases the amount adsorbed. pH 2.0 has been chosen as the optimum pH value for this study to achieve maximum adsorbance.

Kinetic Study

Sorption kinetics is an important physicochemical factor to consider when evaluating a sorption process which can explain the dependency of sorption rates upon the concentrations of sorbate in solution, and how sorption rates are affected by sorption capacity or by the character of the sorbent [24]. The experimental results of biosorption of AO7 on WBY at temperature 303 K and pH 2.0 using different initial dye concentrations are shown in Fig. 3. For all the concentrations of AO7, a larger amount of dyes was removed in the first 20 min of contact time and equilibriums were established in 120 min which was chosen to be the reaction time for further studies. In the initial stage, the surface of WBY is vacant, and the biosorption rate is fast and normally governed by the diffusion process from the bulk solution to the surface. The rapid kinetics has significant practical importance as it will facilitate smaller reactor volumes ensuring efficiency and economy.

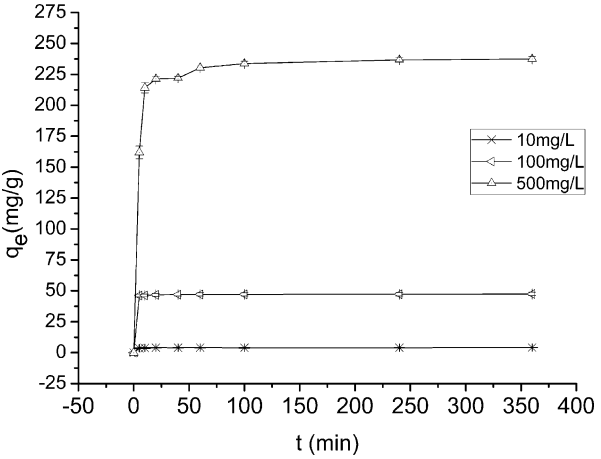

Fig. 3 Effect of initial dye concentration on the adsorption kinetics of AO7 on WBY at pH 2.0, T=303 K

An increase in initial dye concentration led to an increase in the adsorption capacity of dye on WBY and longer time to reach equilibriums. The initial concentration provides an important driving force to overcome all mass transfer resistances between the aqueous and solid phases. Hence a higher initial concentration will enhance the biosorption process. At lower initial concentration, the ratio of molecules of dye to activated sites is lower so the dye molecules can easily and quickly bind to the higher energy activated sites [25]. As the initial concentration increasing, the higher energy activated sites will soon be saturated. Then as the contact time lapse the molecules of dye will be able to bind to the lower energy activated sites or the potential activated sites since the amount of dye molecules is larger and the higher driving force in the higher initial concentration. This will make the time required to reach equilibriums become longer as the initial concentration increased.

Kinetic modeling not only allows estimation of adsorption rates but also leads to suitable rate expressions, characteristic of possible reaction mechanisms. In this respect, the pseudo-first-order and pseudo-second-order adsorption models were used to test kinetic experimental data by nonlinear regression. The nonlinear pseudo-first-order model and nonlinear pseudo-second-order model are showed as follows [26]:

$$\text{Nonlinear pseudo} - \text{first} - \text{order mode}: \; q_t = q_e(1 - e^{-k_1 t}) \tag{2}$$

$$\text{Nonlinear pseudo} - \text{second} - \text{order model}: \; q_t = \frac{q_e^2 k_2 t}{1 + q_e k_2 t} \tag{3}$$

Where q_e and q_t are the amounts of AO7 dye biosorbed at equilibrium and at time t (mg/g), k_1 is the nonlinear pseudo-first-order rate constant (1/min) of biosorption and k_2 is the equilibrium rate constant of nonlinear pseudo-second-order sorption (mg/g min). The kinetic parameters for the biosorption of AO7 dye on WBY are presented in Table 1. Considering the correlation coefficient R^2 in Table 1, for the dye AO7, the experimental data fit pseudo-second-order models better than pseudo-first-order. Thus, the faster second-order model describes experimental data more adequately. The rate constant k decreased as the initial concentration increased while parameter q_e increased which means the time required to reach equilibriums will be longer.

The behavior of adsorption usually involves the mass transfer of a soluble species (adsorbate) from bulk solution to the surface of a solid phase (adsorbent). The transport of adsorbate to adsorbent will occur through four main steps [27]: bulk solution transport, external diffusion, intraparticle diffusion, and adsorption. It is essential for us to understand these mass transfer mechanisms in order to design a cost-effective adsorption system. The steps of bulk transportation and adsorption usually are very rapid so there are rarely to be

Table 1 Values of kinetic parameters for AO7 adsorption on WBY (T=303 K, pH 2.0, initial concentration 10 mg/L to 500 mg/L)

Dye	Initial dye conc. (mg/L)	Pseudo-first order			Pseudo-second order		
		k_1 (min^{-1})	q_{e1} (mg/g)	R^2	k_2 (g·mg^{-1} min^{-1})	q_{e2} (mg/g)	R^2
AO7	10	0.4360	4.048	0.9960	0.3807	4.1086	0.9974
	100	0.3044	46.954	0.9995	0.1604	47.1598	0.9999
	500	0.1063	230.979	0.9942	0.0021	235.2029	0.9955

rate limiting steps. Thus only the external diffusion and intraparticle diffusion are the steps which transportation mechanisms should be concerned.

In the present study, the Spahn and Schlunder model [28] was chosen to describe the external diffusion on the adsorbent

$$\ln\frac{C_t}{C_0} = -k_{\text{ext}}t \tag{4}$$

Where k_{ext} is a constant (1/min). Figure 4 shows the relation between $\ln C_t$ and t with the initial concentration range from 10 mg/L to 500 mg/L at pH 2.0, T=303 K. If the adsorption process is controlled by the external resistance, the plot of $\ln C_t$ versus t should be linear. As shown in the Fig. 4, this kind of relation is obvious for the initial 20 min of the biosorption, which indicates that the external diffusion is the rate-controlling step of the initial fast adsorption at the initial concentration range we investigated.

The intraparticle diffusion model (Weber and Morris [29]) was applied to describe the adsorption at different initial concentrations by WBY. In a liquid–solid system, the fractional uptake of the solute on particle varies according to a function of $[(D_t)^{0.5}/r]^{0.5}$, where D is the diffusivity within the particle and r is the particle radius. The initial of intraparticle diffusion are obtained by linearization of the curve

$$q_t = f(t^{0.5}) \tag{5}$$

The plot of q_t against $t^{0.5}$ may present a multilinearity, which indicates that two or more steps occur in the adsorption process. The first sharper portion is the external surface adsorption or instantaneous adsorption stage. The second portion is the gradual adsorption stage, where the intraparticle diffusion is the rate control. The third portion is final equilibrium stage where the intraparticle diffusion starts to slow down due to extremely low solute concentrations in the solution.

Figure 5 shows the plot of q_t versus $t^{0.5}$ for the adsorption of the AO7 by WBY at different initial concentrations. Since the first stage (external surface adsorption) is completed fast and less apparent because of the instantaneous utilization of the most readily available sites on the adsorbent external surface. Figure 5 only shows the second stage (intraparticle diffusion) and the third stage (equilibrium). The slope of the lines in

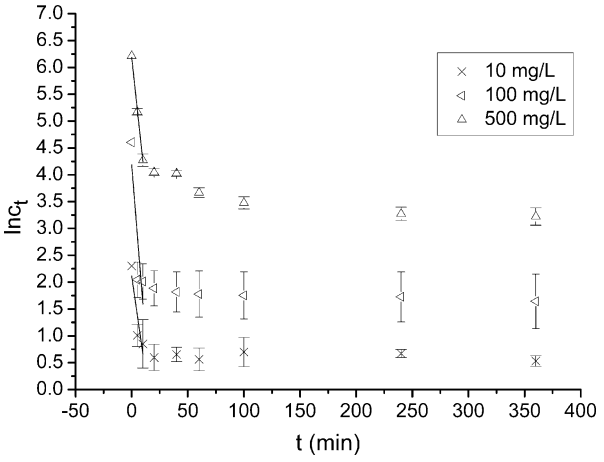

Fig. 4 External diffusion model for adsorption of AO7 on WBY at pH 2.0, T=303 K

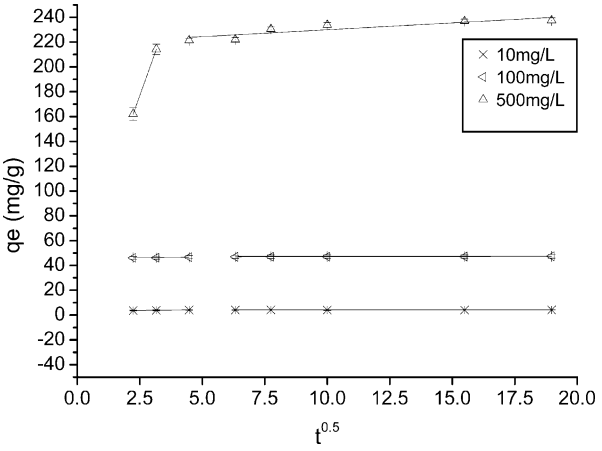

Fig. 5 Intraparticle diffusion model for adsorption of AO7 on WBY at pH 2.0, T=303 K

each stages is defined as the rate parameter $k_{p,i}$ (i=stage number). Rate parameters of the different stages are listed in Table 2.

As seen in Table 2, the order of adsorption rate at the same initial concentration is $k_{p,2}>k_{p,3}$. As mentioned above, initially, the dye was adsorbed by the activated sites of the external surface of the adsorbent, so the adsorption rate was very fast and not shown in this study. When the activated sites of the external surface reached saturation, the dye molecule entered into the pores within the particle and eventually was adsorbed on the active sites of the adsorbent internal surface. When the dye molecule transported in the pore of the particle, the diffusion resistance increased and consequently reduced the diffusion rate. With the decrease of the dye concentration in the solution, the diffusion rate became much smaller and the diffusion processes reached the final equilibrium stage. Rate parameters of the different stages for each dye at different initial concentration also shows that the diffusion rate at different stages increased with the increase of the initial concentration. That may be due to the higher driving force at higher initial dye concentrations thus make the process of diffusion more quickly.

Adsorption Isotherms

Analysis of equilibrium data is important to develop an equation which accurately represents the results and could be used for design purposes. In this study adsorption equilibrium data were fitted to the Langmuir, Freundlich, and Dubinin–Radushkevich (D-R) isotherms at various temperatures.

Table 2 The rate parameters of the different stages for AO7 adsorption on WBY (T=303 K, pH 2.0, initial concentration 10 mg/L to 500 mg/L)

Dye	Initial dye conc. (mg/L)	Intraparticle diffusion	
		K_{p2}(mg·g^{-1}·min$^{-0.5}$)	K_{p3} (mg·g^{-1}·min$^{-0.5}$)
AO7	10	0.2066	0.0042
	100	0.2592	0.0330
	500	56.3965	1.1359

Langmuir isotherm is based on the monolayer adsorption of dyes on the surface of WBY and is expressed in the form as [2]:

$$q_{eq} = \frac{q_{max} b C_{eq}}{1 + b C_{eq}} \tag{6}$$

Where parameters q_{max} and b are Langmuir constants related to maximum adsorption capacity (monolayer capacity) and the free energy of biosorption, C_{eq} is the equilibrium concentration and q_{eq} is the amount adsorbed at equilibrium. q_{max} indicates a practical limiting biosorption capacity when all binding sites are occupied by dye molecules, and allows comparison of biosorption performances. The Langmuir isotherm plots for the AO7 at different temperatures are shown in Fig. 6. The constants derived from nonlinear fit are listed in Table 3. The R^2 in Table 3 suggested that the Langmuir isotherm might be a suitable model for equilibrium data due to the higher correlation coefficients compare to the other models. It was concluded that the biosorption process was monolayer biosorption. The maximum monolayer biosorption capacity for AO7 was increased from 1.94×10^{-3} to 2.27×10^{-3} mol/g as the temperature increased from 293 to 303 K, however, as the temperature further increased from 303 to 313 K the biosorption capacity decreased. This indicates that higher temperature may enhance the biosorption capacity due to the creation of some new biosorption sites or the increased rate of intraparticle diffusion of dye molecule to the pores of the adsorbent. However, a too high temperature may decrease surface activity which resulted in the decreased biosorption capacity as the temperature further increased [30].

Freundlich isotherm describes the heterogeneous surface energies by multilayer adsorption and is expressed in the form of [2]:

$$q_{eq} = K_f C_{eq}^{1/n} \tag{7}$$

Where K_f and n are the Freundlich constants related to adsorption capacity and adsorption intensity, respectively, C_{eq} is the equilibrium concentration and q_{eq} is the amount adsorbed at equilibrium. The Freundlich isotherm plots at different temperatures are shown in Fig. 6, and the constants derived from nonlinear fit are also listed in Table 3. As show in Table 3 the values of n is greater than unity, indicating that the dye is favorably adsorbed by WBY at the temperatures we studied.

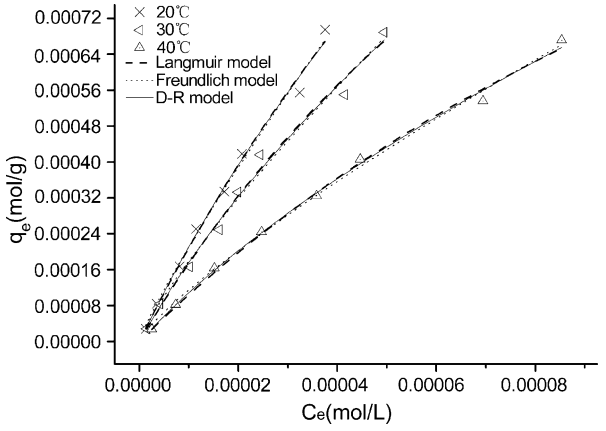

Fig. 6 Different biosorption isotherm plots for the adsorption of AO7at pH 2.0

Table 3 Biosorption isotherm constants for the biosorption of AO7 on WBY at various temperatures T= 303 K, pH 2.0

Dye	T(K)	Langmuir			Freundlich			D-R			E (kJ/mol)
		q_{max} (mol/g)	b (L/mol)	R^2	K_f (mol/g)	n	R^2	q_m (mol/g)	β (mol^2/kJ^2)	R^2	
AO7	293	1.94E−3	10.99E3	0.9929	4.4082	1.17	0.9911	3.45E−3	6.35E−3	0.9928	8.87
	303	2.27 E−3	8.09E3	0.9995	2.2863	1.21	0.9962	2.96E−3	6.12E−3	0.9986	9.04
	313	2.18 E−3	5.00E3	0.9968	1.3801	1.23	0.9965	2.22E−3	5.92E−3	0.9967	9.19

Since the Langmuir and Freundlich isotherm models do not provide any insights into the biosorption mechanism, the equilibrium data were fitted with the D-R isotherm model. The D-R model was used to estimate the mean free energy of biosorption. The form of the D-R model is expressed by [31]

$$q_e = q_m e^{-\beta\varepsilon^2} \tag{8}$$

$$\varepsilon = RT\ln\left(1+\frac{1}{C_e}\right) \tag{9}$$

Where ε is the Polanyi potential, q_m is the biosorption capacity (mol/g), q_e is the amount adsorbed at equilibrium (mol/g), C_e is the equilibrium concentration (mol/L), β is the constant related to the biosorption energy, R is the gas constant and T is the temperature. The D-R plots for AO7 biosorption by WBY is shown in Fig. 6.

The parameters q_m and β can be derived from the nonlinear curve fitting. The mean free energy of sorption (E) is calculated by

$$E = \frac{1}{(2\beta)^{\frac{1}{2}}} \tag{10}$$

The parameters and mean free energy are given in Table 3. The magnitude of E is useful for estimating the type of biosorption process, and the values of E for the biosorption of AO7 were found to range between 8.87 and 9.19 kJ/mol. These values are within energy range of sorption reactions (8–16 kJ/mol). If the interval (8–16 kJ/mol) is taken into consideration, AO7 biosorption by WBY may be classified as chemical sorption [32].

Thermodynamic Analysis of Biosorption

Thermodynamic parameters (energy and entropy) are used to determine whether a biosorption process will spontaneously occur. The Langmuir constants b are used evaluate the standard Gibb's energy by

$$\Delta G = -RT\ln b \tag{11}$$

where b is the Langmuir constant when the concentration term is expressed in L/mol, R is the ideal gas constant (8.314×10^{-3} KJ/mol K), T is the absolute temperature (K).

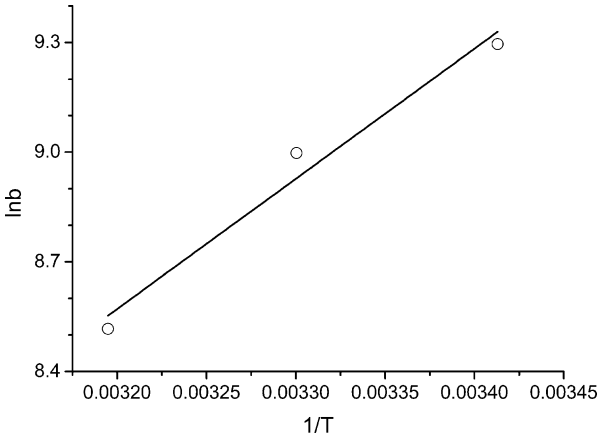

Fig. 7 Van't Hoff plot for AO7 biosorption by WBY

The other thermodynamic parameters such as change in standard enthalpy (ΔH) and standard entropy (ΔS) were determined using the following equation

$$\ln b = \frac{\Delta S}{R} - \frac{\Delta H}{RT} \tag{12}$$

ΔH and ΔS were obtained from the slope and intercept of the Van't Hoff's plot of ln$b$ versus $1/T$ as shown in Fig. 7. Thermodynamic parameters have been evaluated are listed in Table 4. The negative ΔG values indicated that the process of adsorption of AO7 on WBY was feasible and spontaneous. In addition the negative of ΔG value was obtained at 303 K means that which is the optimum temperature for the biosorption of AO7 by WBY, further decreased or increased temperature are not favorable for the process of biosorption at the temperature range we studied. The negative ΔH values indicated exothermic nature of the adsorption. The ΔS parameter was also found to be negative, implying that the AO7 in bulk phase (aqueous solution) were in a much more chaotic distribution compared with the relatively ordered state of solid phase(surface of adsorbent).

Fourier Transform Infrared Spectroscopy

To investigate the main functional groups involved in dyes binding and the chemical nature of the WBY, FT-IR analysis of WBY, and AO7 loaded WBY were studied. The FT-IR spectra of WBY and AO7 loaded WBY are shown in Fig. 8a, b, respectively. As seen from Fig. 8a, the FT-IR spectra of WBY is highly complex, reflecting the complex nature of the WBY. Despite this complexity some characteristic peaks can be assigned. Based on the cell wall composition of yeast, amine or amino, amide, carboxyl, phosphate groups are hypothesized. The spectra of WBY (Fig. 8a) displayed peaks at 3,435 and 1,062 cm^{-1}

Table 4 Thermodynamic parameters for the biosorption of AO7 on WBY

Dye	T(K)	ΔG(kJ/mol)	ΔH(kJ/mol)	ΔS(J/K·mol)
AO7	293	−22.66	−29.59	−23.43
	303	−22.67		
	313	−22.16		

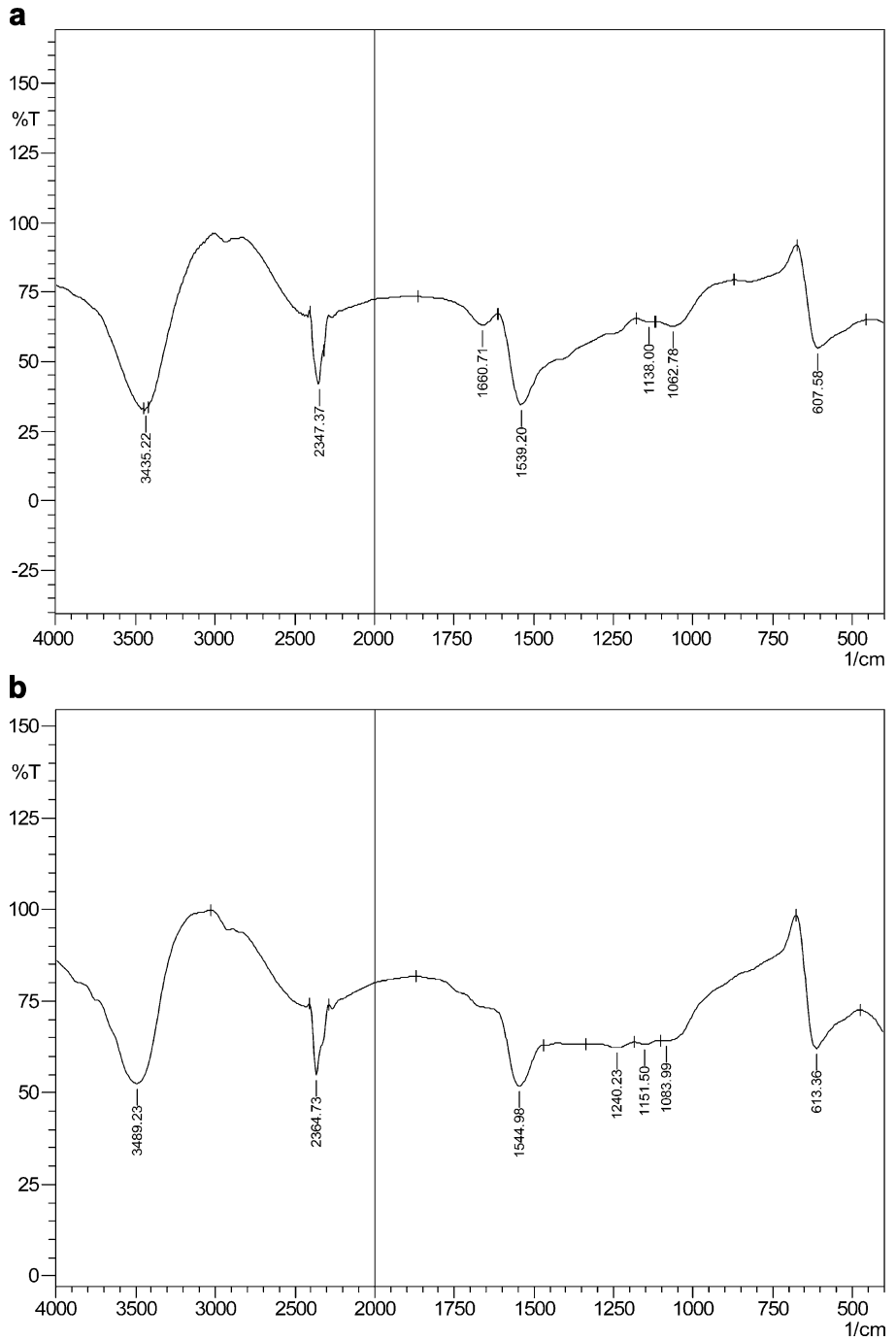

Fig. 8 **a** Fourier transform infrared spectra of WBY. **b** Fourier transform infrared spectra of AO7-loaded WBY

which can be attributed to amino or amine whose characteristic peaks are at 3,500–3,000 cm^{-1}(N–H stretching) and at 1,250–1,000 cm^{-1}(C–N stretching) [33]. Amide group presents characteristic peaks at 3,460–3,400 cm^{-1}(N–H stretching) 1,680–1,630 cm^{-1}(C=O stretching) 1,570–1,510 cm^{-1}(amideIIbond) [34], so peak at 1,660 cm^{-1} and 1,539 cm^{-1} can be assigned amide while N–H stretching is covered. The peaks produced from 3,000–2,500 cm^{-1} are due to carboxylic group [35]. The absorption peaks around 1,138 and 1,062 cm^{-1} (overlapped with C–N stretching of amino) are indicative of *P*=O stretching and P–OH stretching vibrations, respectively [33, 36]. The band between 611 and 520 cm^{-1} represents C–N–C scissoring which is only found in protein structures [37].

Observed from AO7 loaded WBY spectra (Fig. 8b) the location of characteristic peaks of the main functional groups have changed. For example, the characteristic peak of C=O (1,660 cm^{-1}) stretching disappeared, and the peak of *P*=O stretching was shift from 1,138 to 1,151 cm^{-1} after AO7 was loaded. The spectral analysis before and after dyes binding indicated that the amine or amino, amide, carboxyl, phosphate groups are involved in dye binding.

Conclusions

It was concluded that WBY is capable of removing anionic dye AO7 and it can act as a natural, economical, abundant, and effective biosorbent for wastewater treatment. The quantity of eliminated dye was found to depend on pH, and the maximum biosorption of AO7 was found to be at pH 2.0. Kinetic study reveals that the biosorption of AO7 on WBY is quick and the equilibriums were reached within 120 min at all concentration range. The pseudo-second-order rate equation gave the best correlation for the biosorption of AO7 on WBY. Diffusion rate at different stages increased with the increase of the initial concentration. Equilibrium adsorption data at different temperatures fit better with Langmuir model than other models we studied. Based on the Langmuir isotherm model, the optimum temperature for the biosorption of AO7 was 303 K, and it is also supported by the thermodynamic parameters. The biosorption of AO7 by WBY can be classified as chemical sorption when applied the D-R model. The dye-WBY interaction was confirmed by FT-IR analysis and the functional groups on the biosorbent surface such as amine or amino, amide, carboxyl, phosphate were found to play a role in the biosorption process.

Acknowledgments This work is financially supported by the Natural Science Foundation of Hohai University (No. 2009425711).

References

1. Palmieri, G., Cennamo, G., & Sannia, G. (2005). *Enzyme and Microbial Technology, 36*, 17–27.
2. Aksu, Z. (2005). *Process Biochemistry, 40*, 997–1026.
3. Kumar, K. V., Ramamurthi, V., & Sivanesan, S. (2006). *Dyes and Pigments, 69*, 102–107.
4. Amin, N. K. (2009). *Journal of Hazardous Materials, 16*, 552–62.
5. Khataee, A. R., Pourhassan, M., & Ayazloo, M. (2009). *Chinese Journal of Applied and Environmental Biology, 15*, 110–114.
6. Robinson, T., McMullan, G., Marchant, R., & Nigam, P. (2001). *Bioresource Technology, 77*, 247–255.
7. Daneshvar, N., Aleboyeh, A., & Khataee, A. R. (2005). *Chemosphere, 59*, 761–767.
8. Chen, K. C., Wu, J. Y., Liou, D. J., & Hwang, S. C. J. (2003). *Journal of Biotechnology, 101*, 57–68.
9. Ahmad, A. A., Hameed, B. H., & Aziz, N. J. (2007). *Journal of Hazardous Materials, 141*, 70–76.

10. Hasan, M., Ahmad, A. L., & Hameed, B. H. (2008). *Chemical Engineering Journal, 136*, 164–172.
11. Al-Qodah, Z. (2000). *Water Research, 34*, 4295–4303.
12. Hameed, B. H., Mahmoud, D. K., & Ahmad, A. L. (2008). *Colloids and Surfaces A: Physicochemical and Engineering Aspects, 316*, 78–84.
13. Mittal, A., Malviya, A., Kaur, D., Mittal, J., & Kurup, L. (2007). *Journal of Hazardous Materials, 148*, 229–240.
14. Osma, J. F., Saravia, V., Toca-Herrera, J. L., & Couto, S. R. (2007). *Journal of Hazardous Materials, 147*, 900–905.
15. Gupta, V. K., Jain, R., Varshney, S., & Saini, V. K. (2007). *Journal of Colloid and Interface Science, 307*, 326–332.
16. Gupta, V. K., Jain, R., & Varshney, S. (2007). *Journal of Hazardous Materials, 142*, 443–448.
17. Ponnusami, V., Vikram, S., & Srivastava, S. N. (2008). *Journal of Hazardous Materials, 152*, 276–286.
18. Jain, A. K., Gupta, V. K., Bhatnagar, A., & Suhas. (2003). *Journal of Hazardous Materials, B101*, 31–42.
19. Gao, R. Y., Chen, C., & Wang, J. L. (2007). *Journal of Tsinghua University (Science and Technology), 47*, 897–900.
20. Hua, Y., He, B. Y., Peng, H., et al. (2008). *Journal of Hazardous Materials, 158*, 568–576.
21. Padmavathy, V., Vasudevan, P., & Dhingra, S. C. (2003). *Chemosphere, 52*, 1807–1817.
22. Waranusantigul, P., Pokethitiyook, P., Kruatrachue, M., & Upatham, E. S. (2003). *Environmental Pollution, 125*, 385–392.
23. Mittal, A., Kaur, D., & Mittal, J. (2009). *Journal of Hazardous Materials, 163*, 568–577.
24. Akar, S. T., Gorgulu, A., Kaynak, Z., Anilan, B., & Akar, T. (2009). *Chemical Engineering Journal, 148*, 26–34.
25. Karthikeyan, T., & Rajgopal, S. (2005). *Journal of Hazardous Materials, B124*, 192–199.
26. Chiou, M. S., & Chuang, G. S. (2006). *Chemosphere, 62*, 731–740.
27. Wang, X. S., Zhou, Y., Jiang, Y., & Sun, C. (2008). *Journal of Hazardous Materials, 157*, 374–385.
28. Spahn, H., & Schlunder, U. (1975). *Chemical Engineering Science, 30*, 529–537.
29. Weber, W. J., & Morris, J. C. (1963). *Journal of the Sanitary Engineering Division ASCE, 89*, 31–59.
30. Aksu, Z., & Tezer, S. (2000). *Process Biochemistry, 36*, 431–439.
31. Dubinin, M. M., & Radushkevich, L. V. (1947). Proc. Acad. Sci. U.S.S.R. *Physical Chemistry Section, 55*, 331–333.
32. Oguz, E. (2007). *Colloids and Surfaces A, 295*, 258–263.
33. Pangnanelli, F., Papini, P. M., Toro, M., & Veglio, F. (2000). *Environmental Science & Technology, 34*, 2773–2778.
34. Chang, J. H., & Dong, Q. G. (2001). *The principles and analysis of the spectrum* (2nd ed.). Beijing: Science.
35. Nadeem, R., Ansari, T. M., & Khalid, A. M. (2008). *Journal of Hazardous Materials, 156*, 64–73.
36. Arıca, M. Y., & Bayramoglu, G. (2007). *Journal of Hazardous Materials, 149*, 499–507.
37. Bayramoglu, G., Celik, G., & Arica, M. Y. (2006). *Journal of Hazardous Materials, 137*, 1689–1697.